Inorganica Chimica Acta 474 (2018) 66–72

Contents lists available at ScienceDirect

Inorganica Chimica Acta

journal homepage: www.elsevier.com/locate/ica

Research paper

Analysis of the geometrical properties and electronic structure of arsenide doped boron clusters: Ab-initio approach

İskender Muz [a,*], Mustafa Kurban [b], Kazım Şanlı [c]

[a] Department of Mathematics and Science Education, Nevsehir Haci Bektas Veli University, 50300 Nevsehir, Turkey
[b] Department of Electronics and Automation, Ahi Evran University, 40100 Kirşehir, Turkey
[c] Institute of Science, Nevsehir Haci Bektas Veli University, 50300 Nevsehir, Turkey

ARTICLE INFO

Article history:
Received 30 December 2017
Received in revised form 26 January 2018
Accepted 29 January 2018
Available online 01 February 2018

Keywords:
Boron cluster
Arsenide doping
Ab-initio calculation
Electronic structure
Stability

ABSTRACT

Density functional theory (DFT) and coupled-cluster (CCSD(T)) theory have been applied to investigate the geometric, growth pattern, bonding, stability, dissociation, adsorption and electronic properties of arsenide doped boron clusters B_nAs (n = 1–9). Vertical ionization potential (VIP), vertical electron affinity (VEA), HOMO-LUMO energy gap (E_g), binding energy (E_b), chemical hardness (η), and radial distribution functions (RDFs) of B-As and B-B interactions have also been investigated and discussed for the most stable isomers. The results show that the As-dopant atom prefers to locate in peripheral regions for the studied sizes. Arsenic atom can obviously enhance the stability of B_nAs clusters.

1. Introduction

Group-III-arsenides, like BAs, AlAs and GaAs etc., have received considerable attention as potential advanced materials used in many potential applications in electro-optical industry [1–4] due to their desirable physical properties such as wide band gap [5], high melting points [6], dielectric constant [7], high thermal conductivity [8], low ionicity [9,10], short bond length and hardness [11]. Among group-III-arsenide, boron arsenide (BAs) are the most widely studied [12–26] because it has a large mass ratio of constituent atoms, an unusual atomic bonding and a heavy atom (As) having only a single isotope [27]. BAs is found to have a remarkable room temperature thermal conductivity which is comparable to those in diamond and graphite [27].

A large number of investigations on boron clusters and their derivatives doped by other elements have been reported [28–41]. One of the main reasons in these studies is to understand the change of physical properties as a function of size. According to the best of our knowledge, there is no systematic report on an As atom doped B clusters. Therefore it is of importance to accurately calculate the effect of an As atom on the geometries, stabilities, and bonding characteristics of boron clusters by doping of arsenide atom. More interestingly, in order to achieve systematic understanding of the growth pattern and the nature of chemical bonding in large clusters, it is necessary to have a good understanding of small clusters.

In this study, we have investigated the geometry, structural stabilities and electronic properties of the B_nAs (n = 1–9) clusters. In addition, the geometry optimization of the pure boron clusters was calculated by using the same level of theory and basis set to ascertain the effects of the doped arsenide atom on the pure B clusters at the same time. In this regards, we have analysed the optimized average bond lengths, the low-lying isomers with relative energies, binding energy, second-order energy difference, fragmentation energy, vertical ionization potential (VIP), vertical electron affinity (VEA), the highest occupied molecular orbital (HOMO), the lowest unoccupied molecular orbital (LUMO) and the frontier molecular orbital energy gap (HOMO–LUMO difference in energy gap, E_g), chemical hardness (η), the atomic charges of the As atom and radial distribution functions (RDFs) of B-As and B-B binary interactions of the B_nAs (n = 1–9) clusters using density functional theory (DFT) calculations.

2. Computational details

The geometries of low-lying isomers of B_nAs (n = 1–9) clusters are performed using DFT with Becke's three-parameter exchange and Lee–Yang–Parr nonlocal correlation functional (B3LYP) [42].

* Corresponding author.
E-mail addresses: iskender.muz@nevsehir.edu.tr (İ. Muz), mkurbanphys@gmail.com (M. Kurban).

https://doi.org/10.1016/j.ica.2018.01.030
0020-1693/

Before the optimization, in order to get the low-lying energy isomers of B_nAs (n = 1–9) clusters, we considered lots of possible initial geometries obtained by adding or substituting one As atom on the pure B_n and B_{n+1} clusters, which were presented in the previous studies [35,43–46], as well as by adding one B atom to the stable $B_{n-1}As$ clusters. All initial geometries, therefore, were optimized by successively increasing the number of boron by using 3-21G basis set to obtain reliable initial structures. After that, 6-311 + G (2df) basis set was used for further detailed optimization process. The calculations have been performed using the Gaussian09 program package [47]. All optimized geometries are confirmed to be real minima or transition states via frequency computations, which is also used to calculate the zero-point energies (ZPE), at this level of theory. Then, we carry out single point energy (SPE) calculations with coupled-cluster single, double and triple excitation (CCSD(T)) method [48] to get more reliable electronic energies. Although the CCSD(T) method accurately reproduces experimental activation energies [49,50] and electronic properties [51] of various structures, a T1 diagnostic test [52] was also carried out as an additional verification on the quality of the CCSD(T) to estimate possible multireference characters of all of the optimized B_nAs (n = 1–9) clusters. For the lowest-lying isomers of BAs, B_2As and B_6As clusters, we found T1 diagnostic values of 0.067, 0.054 and 0.053, respectively, greater than the threshold value of 0.044 [53], suggesting that a higher-level multireference method is necessary. We have found the T1 diagnostic values for the other clusters in the 0.016–0.036 range, indicating that the clusters are accurately described by the coupled-cluster approach. The 6-311 + G(2df) basis set is also chosen as a compromise between the quality of the theoretical method and the computational cost in the CCSD (T) calculations. The calculations are carried out for singlet-triplet and doublet-quadruplet energy states for considered clusters with even and odd numbers of valance electrons, respectively. All the structures are visualized using the Gauss View 5.0.9 package [54].

3. Results and discussion

3.1. Equilibrium geometries

The obtained results for the lowest-energy structures of the B_n-As (n = 1–9) and pure boron clusters with their corresponding total energies, relative energies (for B_nAs), point group symmetries and electronic states are shown in Fig. 1. The first isomer of the BAs cluster has a linear geometry with $^3\Sigma_G$ electronic state, whereas the second isomer has $^1\Sigma_G$ electronic state. The energy difference between the two isomers is found to be 8.39 kcal/mol, as shown in Fig. 1. In B_2As cluster, the most stable isomer has a triangular geometry with the C_s point group and $^2A'$ electronic state. The second isomer (C_∞,$^2A'$) can be grown from the isomers of the BAs stoichiometry by adding one boron atom. Moreover, the second isomer has 13.82 kcal/mol higher energy than the first isomer. The global minimum of the B_3As cluster has a planar geometry with the C_{2v} point group and the As atom is bonded by B atoms with triangular geometry. The second isomer in this series is reminiscent of the first isomer with C_{2v} point group, whereas it has triplet state (^3A). Moreover, it has a 25.74 kcal/mol higher energy than the global minimum (see in Fig. 1). For B_4As cluster, the first isomer has a "W-shaped planar" geometry with the C_{2v} point group and $^2A'$ electronic state. The second isomer (C_{2v},^2A) can be grown from the first isomer of the B_3As cluster by adding one boron atom, and it has 43.67 kcal/mol higher energy than the first isomer. Up to n = 5, the As doped B_n clusters prefer to grow from the first isomer of the pure boron clusters by adding one arsenide atom. The global minimum of the B_5As has a planar geometry with C_s point group and ^1A electronic state. Moreover, it is a 14.86 kcal/mol lower energy than the second isomer with quasi-planar geometry. The pure boron cluster has a quasi-planar geometry with C_{5v} point group at n = 6, whereas the both isomers of B_6As cluster prefer to planar geometries with C_s point group. It seems obvious that first isomer can be grown from the most stable isomer of the B_5As cluster. The second isomer is also a 7.94 kcal/mol higher energy than the global minimum. The first isomer of the B_7As cluster has an umbrella type geometry with the C_{6v} point group and ^1A electronic state. It can be grown from the lowest isomer of the pure B_7 cluster with one As atom bonded to the B atom in the center of B_7 cluster. Moreover, first time, the As atom prefers to remain on the peripheral position on the below of the cluster. So, it seems that a

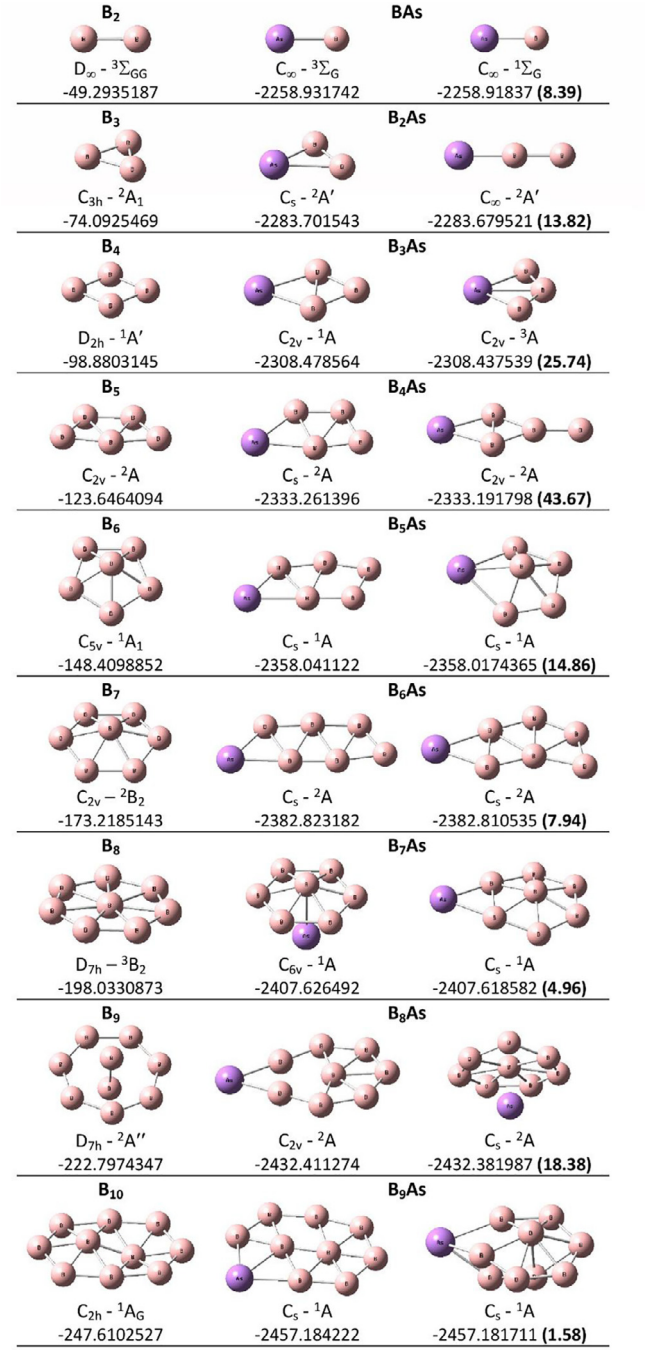

Fig. 1. The low-lying isomers for B_{n+1} and B_nAs (n = 1–9) clusters with relative energies (kcal/mol) at CCSD(T)/6-311 + G(2df)//B3LYP/6-311 + G(2df) without parentheses, at B3LYP/6-311 + G(2df) in parentheses.

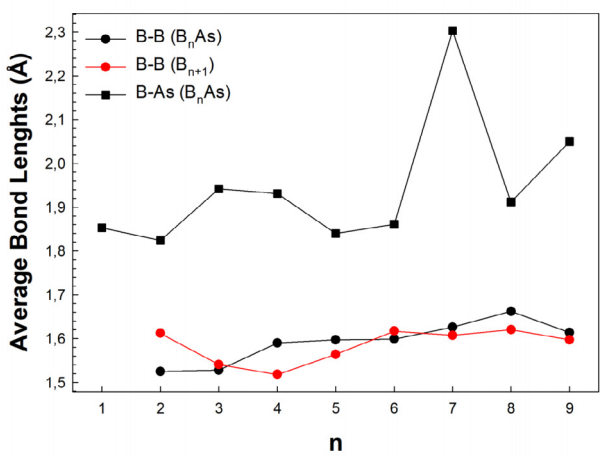

Fig. 2. For the most stable isomers of B_nAs clusters average bond lengths in terms of n.

structural transition from two-dimensional (2D) to three-dimensional (3D) structure. The second isomer of the B_7As cluster has a quasi-planar geometry, and it has a 4.96 kcal/mol higher energy than the first isomer in CCSD(T) level of theory. In B_8As cluster, the first isomer has a configuration with the C_{2v} point group and ^2A electronic state. It is similar to the second isomer of the B_7As cluster. The second isomer of B_8As cluster has a 18.38 kcal/mol higher energy than the first isomer, and it has an umbrella type geometry. Therefore, it can be grown from the global minimum of the B_7As cluster by adding one boron atom. The both isomers of the B_9As cluster have C_s point group and ^1A electronic state. In this series, the first isomer has only 1.58 kcal/mol lower energy than the second isomer.

In Fig. 2, we compared the B-B and B-As average bond lengths for B_nAs and pure boron clusters. There is generally no considerable change in the B-B average bond lengths for both pure boron and As doped B_n clusters with increase the number of boron atoms in the cluster, as seen in Fig. 2. However, the B-As average bond length increases at n = 7 for B_nAs clusters because of a structural transition from 2D to 3D geometry.

3.2. Energetic analysis and relative stability

The relative stability of clusters is performed by computing the various energetic derived. In order to interpret the electronic properties and their evolution as a function of cluster size, we investigated the physical quantities such as the binding energy (E_b) per atom, the second order difference energy $\Delta^2(E)$, the fragmentation or dissociation energy (E_f) of boron atom and the adsorption energy (E_{ads}) of arsenide atom. These quantities can be defined by the following formulas:

$$E_b(B_nAs) = [nE(B) + E(As) - E(B_nAs)]/n + 1 \quad (1)$$

$$E_b(B_n) = [nE(B) - E(B_n)]/n \quad (2)$$

$$\Delta^2(E)(B_nAs) = E(B_{n+1}As) + E(B_{n-1}As) - 2E(B_nAs) \quad (3)$$

$$E_f(B_nAs) = E(B_{n-1}As) + E(B) - E(B_nAs) \quad (4)$$

$$E_{ads} = E(B_n) + E(As) - E(B_nAs) \quad (5)$$

where (B), $E(As)$, $E(B_nAs)$, $E(B_n)$, $E(B_{n+1}As)$ and $E(B_{n-1}As)$ are the total energies of the corresponding atom or cluster.

3.2.1. Binding energy

Variation of the calculated E_b of the most stable isomers of the B_nAs (n = 1–9) clusters in terms of cluster size n are shown in Fig. 3. Also shown in there are the E_b of pure boron cluster. For B_nAs clusters, E_b increases from 2.29 to 4.46 eV in range of n = 1–8, and then follows a plateau at n = 9. Moreover, the dopant As atom obviously contributes to strengthen the stability of B_nAs clusters compared to that of pure counterparts. As increase the number of boron atoms in the cluster, the difference between E_b curves of pure boron and As doped B_n clusters is gradually narrowed. This indicates that the bonding in As doped B_n clusters is actually similar to that of the pure B clusters. We note that the stability of B_nAs can also be related to the stability of pure boron clusters.

3.2.2. The second-order energy difference

In cluster physics, $\Delta^2(E)$ is a sensitive quantity that reflects the relative stability of clusters. Particularly, $\Delta^2(E)$ can compared with the relative abundances determined using mass spectrometry. For B_nAs clusters, the $\Delta^2(E)$ shows odd-even oscillations with a peak for clusters with n even (see Fig. 4). It is interesting note that the

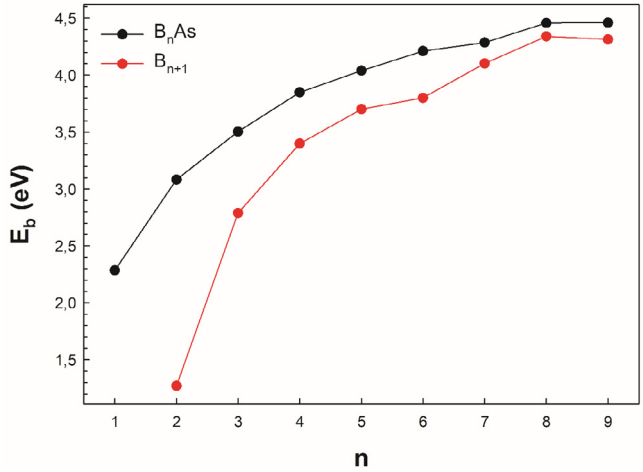

Fig. 3. The binding energy per atom of B_nAs (n = 1–9) clusters in terms of cluster size n.

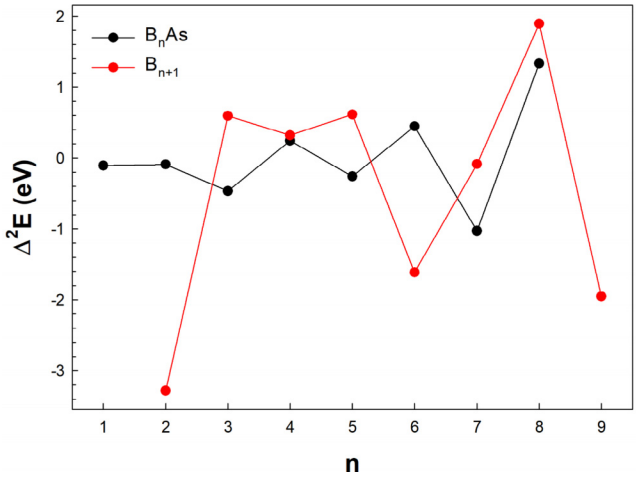

Fig. 4. The second-order energy difference of B_nAs (n = 1–9) clusters as a function of cluster size.

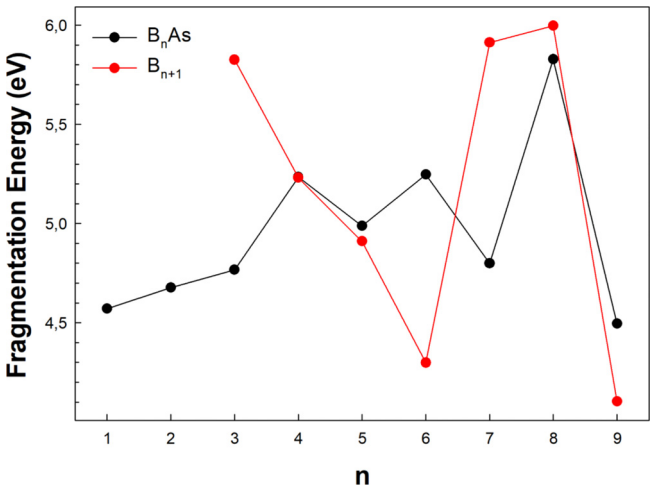

Fig. 5. Variation of the fragmentation energy of the B_nAs (n = 1–9) clusters against the cluster size.

maxima are found at n = 4, 6 and 8, indicating that these clusters have much higher stability than their neighbors. This result is also compatible with the trend of E_b.

3.2.3. Fragmentation energy

The highest fragmentation energies for B_nAs clusters appear at n = 4, 6 and 8, as shown in Fig. 5. One can conclude that these clusters are more stable than their neighboring cluster sizes. Also shown in Fig. 5 are the E_f of pure boron clusters. The local minima of E_f for B_n clusters appears at the sizes of 6 and 9. Additionally when one B is substituted by As atom in B_n clusters, one boron atom in the B_6As and B_9As clusters is more resistant to fragmentation when compared with that of pure B_6 and B_9 cluster.

3.2.4. Adsorption energy

We have also calculated E_{ads}, according to defined as Eq. (5). E_{ads} shows the energy released upon adsorption As from B_nAs clusters. As listed in Table 1, E_{ads} values for the B_nAs clusters change between 4.57 and 6.71 eV in range of n = 1–9. According to our calculations, the BAs cluster has the lowest value of E_{ads} around 4.57 eV. The largest values for E_{ads} of 6.71 and 6.68 eV are found for B_2As and B_6As, respectively.

3.3. Electronic structure analysis

The electronic structure of clusters can be verified through experimental measurements of such as vertical ionization potential (VIP), vertical electron affinity (VEA), the highest occupied

Table 1
Binding energy per atom (E_b), the fragmentation or dissociation energy of B atom (E_f), the adsorption energy of As atom (E_{ads}), vertical ionization potential (VIP), vertical electron affinity (VEA), HOMO-LUMO energy gap (E_g) and chemical hardness (η) calculated at B3LYP/6-311 + G(2df) level of theory. All values are in eV.

Structure	E_b/atom	E_f	E_{ads}	VIP	VEA	E_g	η
B_1As	2.29	4.57	4.57	9.96	2.60	8.29	3.73
B_2As	3.08	4.68	6.71	9.02	1.48	9.76	3.87
B_3As	3.50	4.77	5.65	8.17	1.78	7.70	3.38
B_4As	3.85	5.23	5.65	8.06	2.60	8.34	2.97
B_5As	4.04	4.99	5.73	7.90	2.98	7.21	2.78
B_6As	4.21	5.25	6.68	7.99	2.91	2.79	2.93
B_7As	4.29	4.80	5.56	7.91	1.27	4.59	3.82
B_8As	4.46	5.83	5.40	7.63	3.87	1.93	2.41
B_9As	4.46	4.49	5.79	7.50	3.27	2.80	3.11

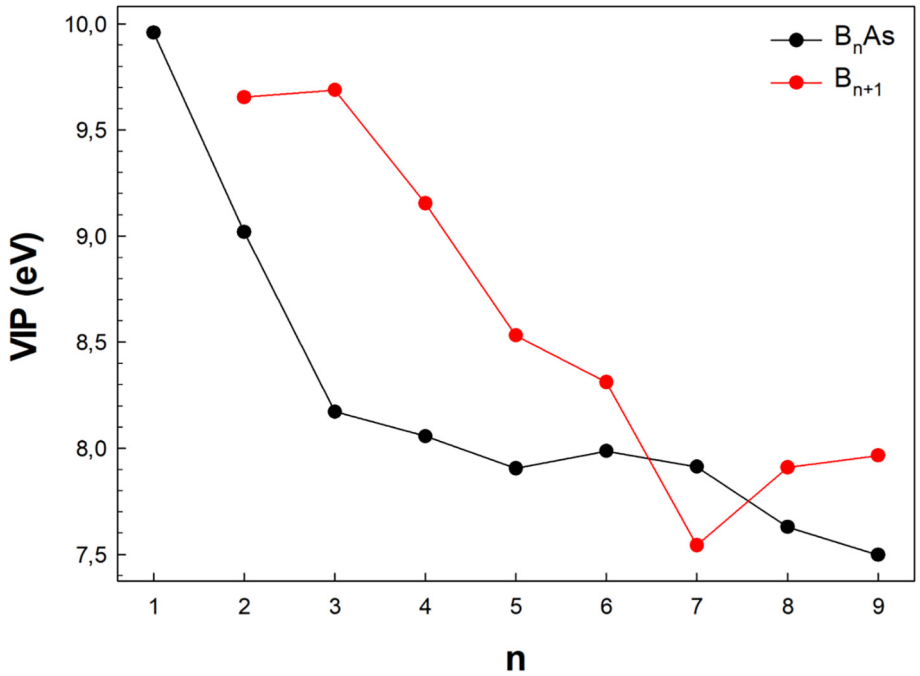

Fig. 6. Size dependence of vertical ionization potential (VIP) for the most stable isomers of the B_nAs (n = 1–9) clusters.

molecular orbital (HOMO)–lowest unoccupied molecular orbital (LUMO) gap (E_g), chemical hardness (η) and charge analysis etc. Therefore, we also investigated these quantities to interpret the electronic properties and their evolution as a function of cluster size. These quantities can be defined by the following formulas:

$$VIP(B_nAs) = [E(B_nAs)cation] - [E(B_nAs)neutral] \quad (6)$$

$$VEA(B_nAs) = [E(B_nAs)neutral] - [E(B_nAs)anion] \quad (7)$$

where VIP and VEA, which optimized by the geometry of the neutral, the energy difference between the ground state of the cation and the ground state of the neutral and the energy difference between the ground state of the anionic and the neutral clusters, respectively. The VIP is plotted in Fig. 6 and listed in Table 1. For B_n-As clusters, the VIP decreases (from 9.99 eV to 7.90 eV) sharply up to n = 5. After small increase (7.99 eV) at n = 6, it again decreases (up to 7.50 eV) in range of n = 7–9. However, when one B is substituted by As atom in B_n clusters VIPs have lower than the corresponding B_n clusters, except for BAs and B_7As clusters. For VEA, there is no general trend in B_nAs clusters, but the local minimums are found at n = 2, 7 indicating that these clusters have much lower stability than their neighbors (see Fig. 7 and Table 1). However, the odd-even oscillations are generally observed in pure B_n clusters. As seen in Fig. 7, the VEAs of B_nAs are higher than those of B_n clusters except for B_nAs at n = 3 and 7.

E_g results are showed in Fig. 8. For B_nAs clusters, E_g shows a decrease trend with odd-even oscillations in range of n = 1–5 and

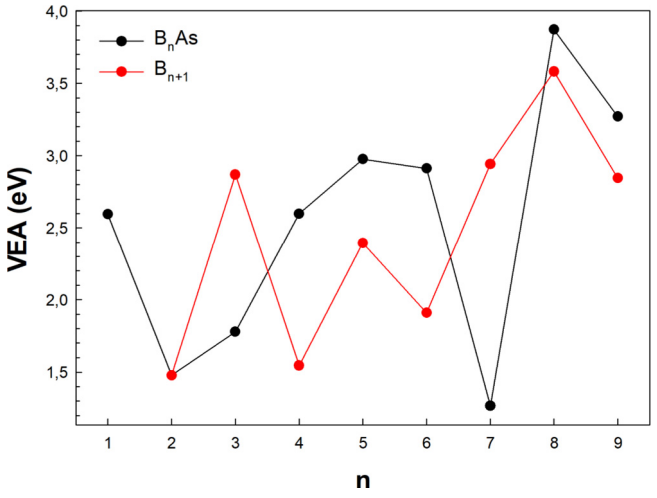

Fig. 7. Size dependence of vertical electron affinity (VEA) for the most stable isomers of the B_nAs (n = 1–9) clusters.

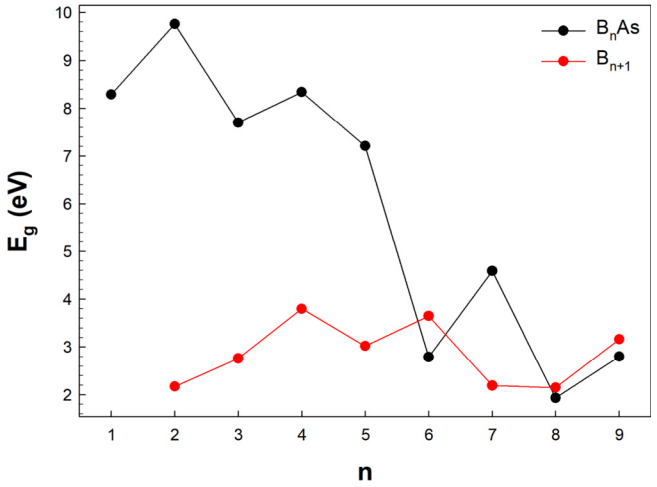

Fig. 8. Variation of the HOMO–LUMO gaps of the B_nAs (n = 1–9) clusters against the cluster size.

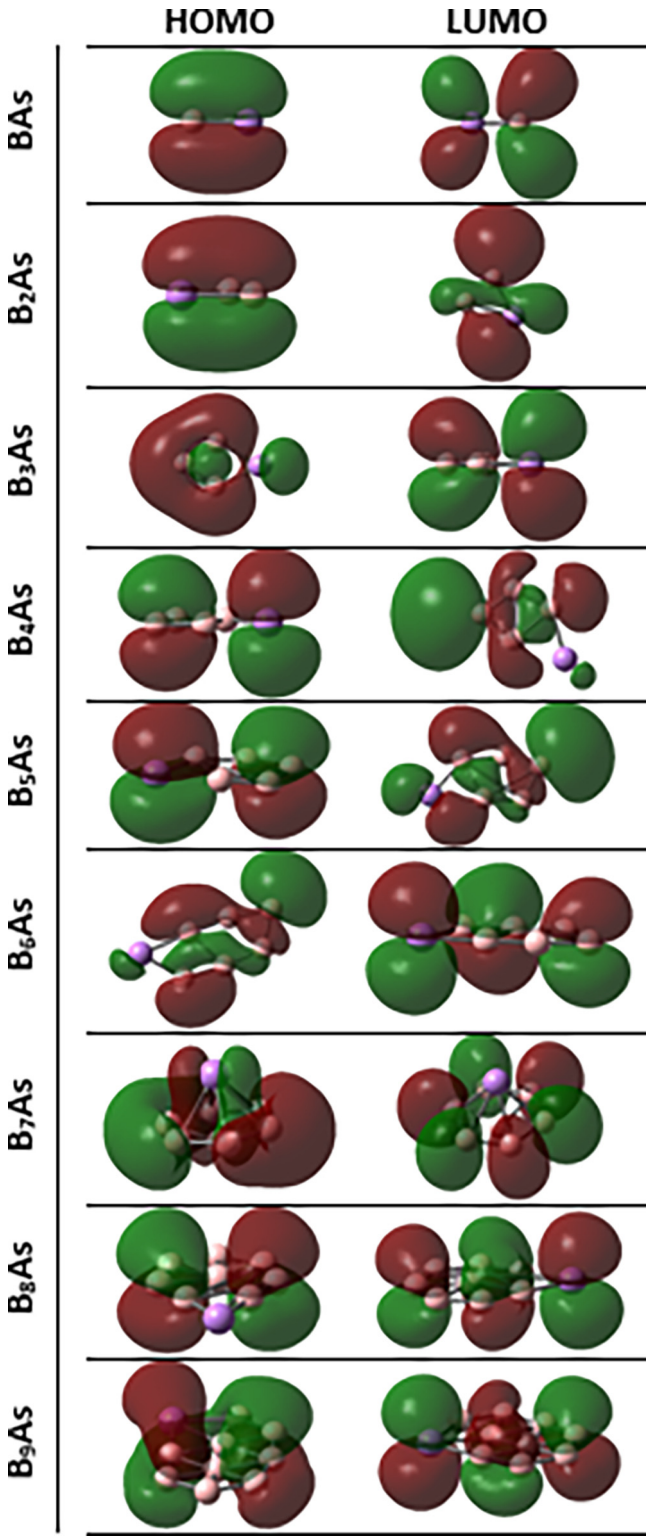

Fig. 9. HOMO and LUMO pictures of the B_nAs (n = 1–9) clusters. Green and red colors represent the positive and negative isosurfaces for HOMO and LUMO, respectively. (For interpretation of the references to colour in this figure legend, the reader is referred to the web version of this article.)

thus the energy difference will cause higher inhibition efficiency. After that, it decreases (up to 2.79 eV) sharply at n = 6, and then again exhibit odd–even oscillations with a peak for n = 7. As seen in Fig. 8, E_g values of B_nAs are higher than those of B_n clusters except at n = 6 and 8. HOMO and LUMO pictures of the B_nAs (n = 1–9) clusters are shown in Fig. 9. HOMO and LUMO localizations are found to be almost symmetric over the structures.

Another useful quantity is the chemical hardness [55], which can be approximated as

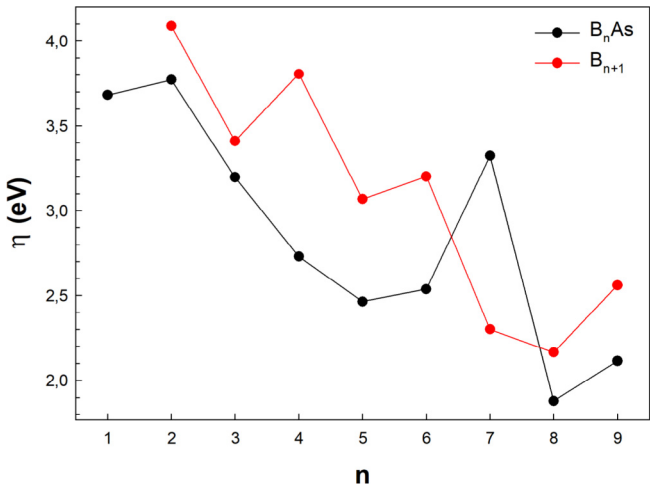

Fig. 10. Variation of chemical hardness (η) of the most stable isomers of the B_nAs (n = 1–9) clusters.

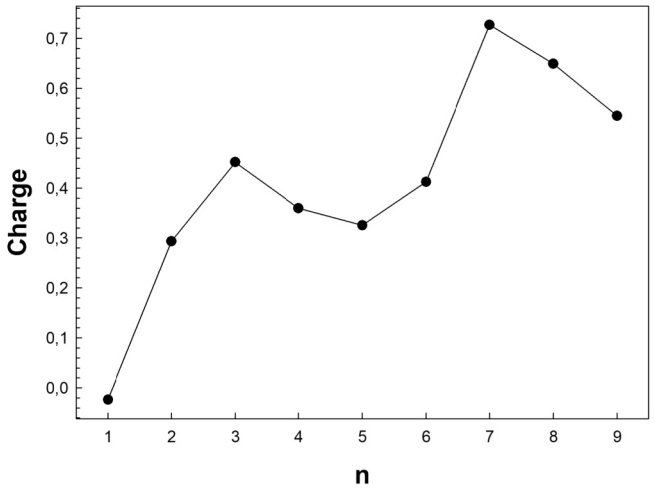

Fig. 11. Variation of the atomic charges of the As atom in the B_nAs clusters depending on size n.

$$\eta \approx 1/2(VIP - VEA) \quad (8)$$

For B_nAs clusters, η decreases generally except for B_7As cluster as a function of the cluster size (see Fig. 10). However, η of B_nAs clusters are smaller than those of pure boron clusters except for n = 7. We also note that, η curve exhibits a decreasing trend similar to E_g.

Natural population analysis is also performed in this study. The atomic charges of the As atom in the B_nAs clusters depending on size n are shown in Fig. 11. The charges for both As and B atoms in the B_nAs clusters are listed in Table 2. The charge on As in the B_nAs clusters is positive in range of n = 2–9, so As atom contributes its electronic charges in the nearest neighboring boron atoms. Therefore, charge always transfers from As to B atoms with the increase of size n. This result means that As atom acts as an electron donor in B_nAs clusters except for BAs cluster.

3.4. Radial distribution function

Fig. 12 shows the radial distribution functions (RDFs) analysis for the boron-boron (B-B), and boron-arsenide (B-As) interactions of (a) B_4As, (b) B_5As, (c) B_6As, (d) B_7As, (e) B_8As and (f) B_9As clusters. The RDFs is calculated for each atomic pairs of the most stable isomers of the B_nAs (n = 4–9) clusters. One can see that B-As has a narrower and higher distribution for B_7As cluster than the other pair interactions because of the weaker bond between B and As. B-B interactions for B_4As B_6As and B_9As clusters are higher distribution than that of B_5As, B_7As and B_8As clusters. In addition, behavior of B-B and B-As interactions is quite different from each other. For B atoms, B-As for B_9As cluster is shorter than the interactions in the other clusters. For all of the combinations in the clusters, B-As for B_7As cluster has stronger interactions than the other ones.

4. Conclusions

We performed a systematic investigation on arsenide doped boron B_nAs (n = 1–9) clusters using density functional (DFT) and coupled-cluster (CCSD(T)) theories. The dopant As atom prefers to occupy a peripheral position for the studied sizes. The presence of As dopant obviously enhances the stability of B_nAs clusters compared to that of pure counterparts. The HOMO-LUMO energy gap values exhibit a decreasing trend similar to the chemical hardness. However, the chemical hardness of B_nAs clusters are smaller than those of pure boron clusters except n = 7. The results of the fragmentation energy and the second-order difference energy indicate that the B_nAs (n = 4, 6 and 8) clusters are more stable than their neighbors. According to VIP, VEA, HOMO and LUMO values, B_7As structure has a high tendency to donate electrons and has low energy required to break the electrons, so it is more unstable than the others. The dopant As atom interacting with boron atoms affects the electronic properties of boron clusters. In addition,

Table 2
Natural populations of the As and B atoms of the most stable B_nAs (n = 1–9) clusters.

Structure	As	B(1)	B(2)	B(3)	B(4)	B(5)	B(6)	B(7)	B(8)	B(9)
B_1As	−0.02	0.02								
B_2As	0.29	−0.36	0.06							
B_3As	0.45	−0.26	−0.26	0.06						
B_4As	0.36	−0.11	−0.30	0.18	−0.13					
B_5As	0.33	−0.13	−0.25	−0.07	−0.10	0.22				
B_6As	0.41	−0.09	−0.14	−0.11	−0.12	−0.20	0.24			
B_7As	0.73	−0.22	−0.08	−0.08	−0.08	−0.08	−0.08	−0.08		
B_8As	0.65	−0.12	0.05	0.20	0.09	0.20	0.05	−0.31	−0.31	
B_9As	0.54	−0.46	−0.16	0.12	0.09	0.16	0.01	−0.03	−0.02	−0.24

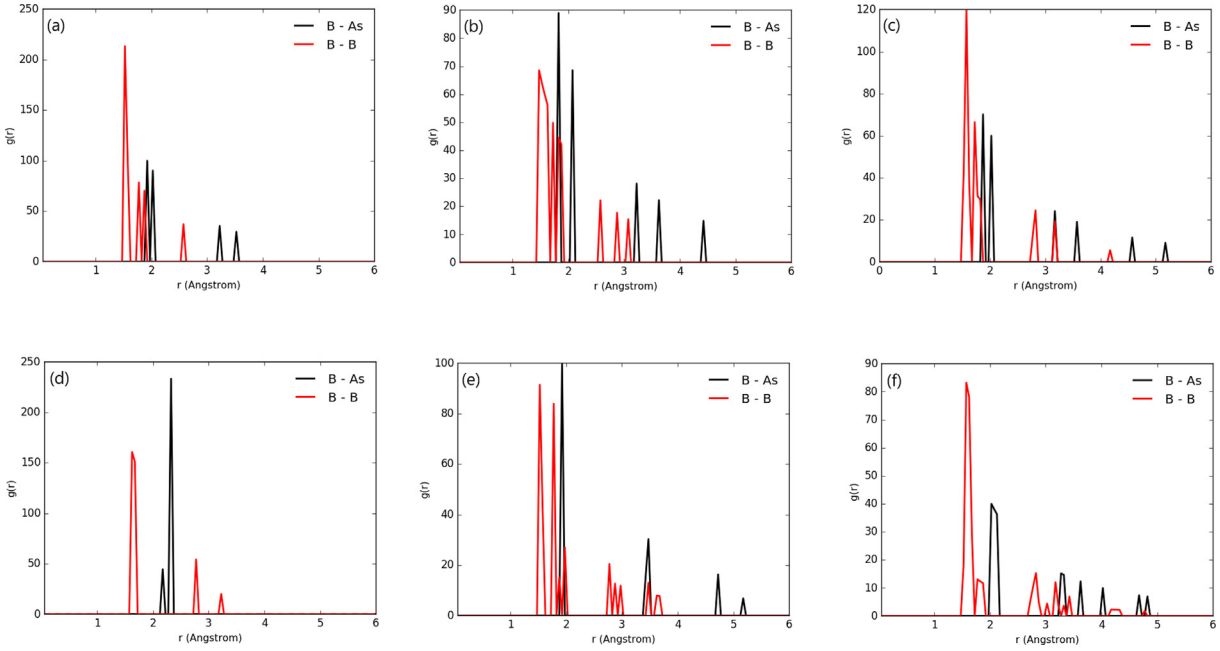

Fig. 12. The radial distribution functions (RDFs) of the boron-boron (B-B), and boron-arsenide (B-As) interactions of (a) B_4As, (b) B_5As, (c) B_6As, (d) B_7As, (e) B_8As and (f) B_9As clusters.

B-As interactions have a narrower and higher distribution for B_7As cluster due to a structural transition from 2D to 3D geometry.

Acknowledgments

This work was supported by the Ahi Evran University Scientific Research Projects Coordination Unit. Project Number: TBY. C1.17.001, Turkey.

References

[1] R. Ahmed, S. Javad Hashemifar, H. Akbarzadeh, M. Ahmed, Fazal-e-Aleem, Comput. Mater. Sci. 39 (2007) 580.
[2] A. Zaoui, S. Kacimi, A. Yakoubi, B. Abbar, B. Bouhafs, Phys. B-Condens. Matter 367 (2005) 195.
[3] D. Touat, M. Ferhat, A. Zaoui, J. Phys.-Condens. Matter 18 (2006) 3647.
[4] S. Cui, W. Feng, H. Hu, Z. Feng, Y. Wang, Comput. Mater. Sci. 44 (2009) 1386.
[5] M.P. Surh, S.G. Louie, M.L. Cohen, Phys. Rev. B 43 (1991) 9126.
[6] O.A. Golikova, Phys. Status Solidi 51 (1979) 11.
[7] I. Vasiliev, S. Ogut, J.R. Chelikowsky, Phys. Rev. Lett. 78 (1997) 4805.
[8] B. Lv, Y. Lan, X. Wang, Q. Zhang, Y. Hu, A.J. Jacobson, D. Broido, G. Chen, Z. Ren, C.-W. Chu, Appl. Phys. Lett. 106 (2015) 074105.
[9] A. Garcia, M.L. Cohen, Phys. Rev. B 47 (1993) 4215.
[10] M. Ferhat, A. Zaoui, M. Certier, H. Aourag, Phys. B 252 (1998) 229.
[11] R.M. Wentzcovitch, M.L. Cohen, P.K. Lam, Phys. Rev. B 36 (1987) 6058.
[12] H. Ma, C. Li, S. Tang, J. Yan, A. Alatas, L. Lindsay, B.C. Sales, Z. Tian, Phys. Rev. B 94 (2016) 220303(R).
[13] I.H. Nwigboji, Y. Malozovsky, L. Franklin, D. Bagayoko, J. Appl. Phys. 120 (2016) 145701.
[14] N.H. Protik, J. Carrete, N.A. Katcho, N. Mingo, D. Broido, Phys. Rev. B 94 (2016) 045207.
[15] J. Kim, D.A. Evans, D.P. Sellan, O.M. Williams, E. Ou, A.H. Cowley, L. Shi, Appl. Phys. Lett. 108 (2016) 201905.
[16] R. Zhang, C. Zhang, W. Ji, S. Li, P. Wang, S. Hu, S. Yan, Appl. Phys. Express 8 (2015) 113001.
[17] S. Daoud, N. Bioud, N. Bouarissa, Mater. Sci. Semicond. Process. 31 (2015) 124.
[18] V.G. Hadjiev, M.N. Iliev, B. Lv, Z.F. Ren, C.W. Chu, Phys. Rev. B 89 (2014) 024308.
[19] D.A. Broido, L. Lindsay, T.L. Reinecke, Phys. Rev. B 88 (2013) 214303.
[20] I. Magoulas, A. Kalemos, J. Chem. Phys. 139 (2013) 154309.
[21] L. Lindsay, D.A. Broido, T.L. Reinecke, Phys. Rev. Lett. 111 (2013) 025901.
[22] C.E. Whiteley, M.J. Kirkham, J.H. Edgar, J. Phys. Chem. Solids 74 (2013) 673.
[23] S. Wang, S.F. Swingle, H. Ye, F.-R.F. Fan, A.H. Cowley, A.J. Bard, J. Am. Chem. Soc. 134 (2012) 11056.
[24] J. Wu, H. Zhu, D. Hou, C. Ji, C.E. Whiteley, J.H. Edgar, Y. Ma, J. Phys. Chem. Solids 72 (2011) 144.
[25] Y. Gong, Y. Zhang, M. Dudley, Y. Zhang, J.H. Edgar, P.J. Heard, M. Kuball, J. Appl. Phys. 108 (2010) 084906.
[26] Y. Gong, M. Tapajna, S. Bakalova, Y. Zhang, J.H. Edgar, Y. Zhang, M. Dudley, M. Hopkins, M. Kuball, Appl. Phys. Lett. 96 (2010) 223506.
[27] L. Lindsay, D.A. Broido, T.L. Reinecke, PRL 111 (2013) 025901.
[28] E.K. Yildirim, Int. J. Mod. Phys. B 29 (2015) 1550172.
[29] J. Gu, C. Wang, Y. Cheng, L. Zhang, X. Yang, Comput, Theor. Chem. 1049 (2014) 67.
[30] G. Yang, W. Cui, X. Zhu, R. Yue, J. Mol. Model. 20 (11) (2014) 2482.
[31] J. Jia, L. Ma, J.-F. Wang, H.-S. Wu, J. Mol. Model. 19 (2013) 3255.
[32] G. Jian-Bing, Y. Xiang-Dong, W. Huai-Qian, L. Hui-Fang, Chin. Phys. B 21 (2012) 043102.
[33] R. Shi, J. Shao, C. Wang, X. Zhu, X. Lu, J. Mol. Model. 17 (2011) 1007.
[34] T.B. Tai, P. Kadlubanski, S. Roszak, D. Majumdar, J. Leszczynski, M.T. Nguyen, ChemPhysChem 12 (2011) 2948.
[35] T.B. Tai, M.T. Nguyen, Chem. Phys. 375 (2010) 35.
[36] L. Xue-Ling, Z. Heng-Jiang, G. Gui-Xian, W. Xian-Ming, L. You-Hua, ACTA Phys. Sin. 57 (2008) 5491.
[37] Z. Yang, S.-J. Xiong, J. Chem. Phys. 128 (2008) 184310.
[38] J.-G. Yao, X.-W. Wang, Y.-X. Wang, Chem. Phys. 351 (2008) 1.
[39] X. Liu, G. Zhao, L. Guo, Q. Jing, Y. Luo, Phys. Rev. A 75 (2007) 063201.
[40] R. Wang, D. Zhang, R. Zhu, C. Liu, J. Mol. Struct. 817 (2007) 119.
[41] D.T.T. Mai, L. Van Duong, T.B. Tai, M.T. Nguyen, J. Phys. Chem. A 120 (2016) 3623.
[42] A.D. Becke, J. Chem. Phys. 98 (1993) 5648.
[43] N. Akman, M. Tas, C. Ozdogan, I. Boustani, Phys. Rev. B 84 (2011) 075463.
[44] M. Atis, C. Ozdogan, Z.B. Guvenc, Int. J. Quantum Chem. 107 (2007) 729.
[45] I. Boustani, Phys. Rev. B 55 (1997) 16426.
[46] L. Li-Ren, L. Xue-Ling, C. Hang, Z. Heng-Jiang, Acta Phys. Sin. 58 (2009) 5355.
[47] M.J. Frisch, G.W. Trucks, H.B. Schlegel, G.E. Scuseria, M.A. Robb, J.R. Cheeseman, G. Scalmani, V. Barone, B. Mennucci, G.A. Petersson, H. Nakatsuji, M. Caricato, X. Li, H.P. Hratchian, A.F. Izmaylov, J. Bloino, G. Zheng, J.L. Sonnenberg, M. Hada, M. Ehara, K. Toyota, R. Fukuda, J. Hasegawa, M. Ishida, T. Nakajima, Y. Honda, O. Kitao, H. Nakai, T. Vreven, J.A. Montgomery Jr., J.E. Peralta, F. Ogliaro, M. Bearpark, J.J. Heyd, E. Brothers, K.N. Kudin, V.N. Staroverov, R. Kobayashi, J. Normand, K. Raghavachari, A. Rendell, J.C. Burant, S.S. Iyengar, J. Tomasi, M. Cossi, N. Rega, J.M. Millam, M. Klene, J.E. Knox, J.B. Cross, V. Bakken, C. Adamo, J. Jaramillo, R. Gomperts, R.E. Stratmann, O. Yazyev, A.J. Austin, R. Cammi, C. Pomelli, J.W. Ochterski, R.L. Martin, K. Morokuma, V.G. Zakrzewski, G.A. Voth, P. Salvador, J.J. Dannenberg, S. Dapprich, A.D. Daniels, Ö. Farkas, J.B. Foresman, J. V Ortiz, J. Cioslowski, D.J. Fox, Gaussian~09 {R}evision {E}.01, Gaussian Inc., Wallingford CT 2009, (n.d.).
[48] K. Raghavachari, G.W. Trucks, J.A. Pople, M. Headgordon, Chem. Phys. Lett. 157 (1989) 479.
[49] B.M. Wong, S. Raman, J. Comput. Chem. 28 (2007) 759.
[50] B.M. Wong, A.H. Steeves, R.W. Field, J. Phys. Chem. B 110 (2006) 18912.
[51] M.B. Oviedo, N.V. Ilawe, B.M. Wong, J. Chem. Theory. Comput. 12 (2016) 3593.
[52] T.J. Lee, P.R. Taylor, Int. J. Quantum Chem. 36 (1989) 199.
[53] S. Pari, I.A. Wang, H. Liu, B.M. Wong, Environ. Sci.: Processes 19 (2017) 395.
[54] R. Dennington, T.A. Keith, J.M. Millam, GaussView V version {5.0.9}, (2009).
[55] R.G. Parr, R.G. Pearson, J. Am. Chem. Soc. 105 (1983) 7512.